

This leads to a nonvanishing phonon density of states at $k = 0$ and therefore to strong elastic scattering by the isotopic disorder and to disorder induced linewidth (FWHM) increases of $\sim 6 \text{ cm}^{-1}$ for diamond of $^{12}\text{C}_{0.6}^{13}\text{C}_{0.4}$ composition. The corresponding effect in germanium (for $^{70}\text{Ge}_{0.5}^{76}\text{Ge}_{0.5}$) is only 0.04 cm^{-1} [14].

Recent developments in progress include the growth of isotopic superlattices [14]. Work is in progress for the $^{70}\text{Ge}^{74}\text{Ge}$ system (which is also of interest because it can be doped p-n through nuclear transmutation [15]) and also for $^{69}\text{GaAs}/^{71}\text{GaAs}$ [16]. Phonons confined or partially confined in each of the isotopic layers have been observed by Raman scattering [17]. They yield a great deal of information on the lattice dynamics and the scattering mechanism.

I would like to thank G. Abstreiter, T. Anthony, and E.E. Haller for supplying the samples discussed here and P.G. Etchehoin for a careful reading of the manuscript.

- [1] K. Itoh et al., *J. Mater. Res.* **8**, 1341 (1993).
- [2] R.C. Buschert et al., *Phys. Rev. B* **38**, 5219 (1993); H. Holloway et al., *Phys. Rev. B* **44**, 7123 (1991).
- [3] J.R. Olson et al., *Phys. Rev. B* **47**, 14850 (1993).
- [4] A.K. Ramdas et al., *Phys. Rev. Lett.* **71**, 189 (1993).
- [5] J. Spitzer et al., *Solid State Commun.* **88**, 509 (1993).
- [6] H.D. Fuchs et al., *Phys. Rev. Lett.* **70**, 1715 (1993).
- [7] P. Etchehoin et al., *Phys. Rev. B* **48**, 12661 (1993).
- [8] K.C. Hass et al., *Phys. Rev. B* **44**, 12046 (1991).
- [9] H.D. Fuchs et al., *Phys. Rev. B* **44**, 8633 (1991).
- [10] A.T. Collins et al., *Phys. Rev. Lett.* **65**, 891 (1990).
- [11] P. Etchehoin et al., *Solid State Commun.* **83**, 843 (1992); G. Davies et al., *Semicond. Sci. and Technol.* **7**, 1271 (1992).
- [12] V.F. Agekyan et al., *Sov. Phys. Solid State* **31**, 2082 (1989).
- [13] P. Pavone et al., *Phys. Rev. B* **48**, 3156 (1993).
- [14] M. Cardona et al., *J. Phys.* **33A**, A61 (1993).
- [15] E.E. Haller, *Semicond. Sci. Technol.* **5**, 319 (1990).
- [16] T.Y. Tan et al., *J. Appl. Phys.* **72**, 5206 (1992).
- [17] J. Spitzer et al., *Phys. Rev. Lett.*, in press.

"Electronic Dephasing in Femtosecond Curve Crossing Spectroscopy," Y. Tanimura and S. Mukamel, in *Proceedings of the XIVth International Conference on Raman Spectroscopy*, N.-T. Yu and X.-Y. Li, Eds. (Wiley, New York) (1994) pp. 23 - 26.

ELECTRONIC DEPHASING IN FEMTOSECOND CURVE CROSSING SPECTROSCOPY

Y. Tanimura^{1,2} and S. Mukamel^{1*}

¹Department of Chemistry, University of Rochester, Rochester, New York 14627

²Institute for Molecular Science, Myodaiji, Okazaki 444, Japan

Femtosecond nonlinear optical spectroscopies provide a powerful tool for studying electronic and vibrational dynamics, including nonadiabatic curve crossing and electron transfer processes. In this paper we outline a procedure for incorporating microscopically effects of electronic dephasing in coherent spectroscopies involving strong fields. The approach applies to coherent Raman measurements as well as any other four wave mixing including pump-probe spectroscopy. It is based on equations of motion for phase space wavepackets, and provides a simple semiclassical picture for these processes.

We consider a molecular system with electronic states denoted $|j\rangle$. The Hamiltonian of the system is

$$H_S(t) = \frac{P^2}{2M} + \sum_j |j\rangle U_j(R, t) \langle j|, \quad (1)$$

Here, R is a nuclear coordinate strongly coupled to the electronic state and P is its conjugate momentum. The potential of j th state is denoted by U_j which may depend on time. The system interacts with optical field and the total Hamiltonian is

$$H_A(t) = H_S(t) + \sum_k \frac{\hbar}{2} (E_k(r, t) + E_k^*(r, t)) \mu_k(R) |j\rangle \langle k|, \quad (2)$$

where $E_j(r, t)$ is a strong field that can represent a sequence of pulses with arbitrary time profile and $E_k(r, t)$ is a weak field hereby denoted the "probe". In the following calculations the optical signal will be calculated to lowest order in $E_k(r, t)$ but to arbitrary order in $E_j(r, t)$. The transition dipole matrix element between the j and k states which may depend on R (non-Condon effects) is given by $\mu_k(R)$.

Optical measurements can be calculated from the polarization

$$P(r, t) \equiv \text{tr}[\mu(R) \hat{\rho}(r, t)], \quad (3)$$

where $\mu(R) = \sum_k \mu_k(R) |j\rangle \langle k|$ and $\hat{\rho}(r, t)$ is the total density matrix. We next expand the polarization in momentum (k) space

$$P(r, t) = \sum_j \exp[ik_j r - i\Omega_j t] P(k_j, t), \quad (4)$$

Optical measurements are most commonly carried out using one of the following two detection schemes. First, in *homodyne* detection one simply measure the outgoing field in a specified direction k_j :

$$(i) \quad S(k_j, t) = P(k_j, t)^2. \quad (5)$$

Second, in the *heterodyne* detection mode, the outgoing field is mixed with a reference field denoted the local oscillator E_{loc} , and the signal is given by

$$(ii) \quad S(k_j, t) = \text{Im}[E_{loc}(k_j, t)P(k_j, t)]. \quad (6)$$

Example of (i) are four wave mixing and coherent Raman which is observed in the $k_j = 2k_1 - k_2$ direction, whereas pump-probe experiment with $k_j = k_1 - k_1 + k_2$ corresponds to heterodyne detection.

Let us recast the Hamiltonian in the form,

$$H_A(t) = \frac{P^2}{2M} + \sum_j \sum_k |j\rangle \langle j| U_{jk}(R, t) \langle k|, \quad (7)$$

where we set $U_{jk}(R, t) \equiv \langle j| \mu_{jk}(R)(E_j(\mathbf{r}, t) + E_k(\mathbf{r}, t)) \rangle$. The multi-state density matrix in the nuclear phase space (The Wigner representation) is expanded as

$$\hat{\rho}(t) = \sum_{j,k} |j\rangle \langle j| W_{jk}(P, R, t) \langle k|. \quad (8)$$

The Wigner representation has the following advantages; first it allows us to compare the quantum density matrix directly with its classical counterpart. Second, using phase space distribution functions, we can further easily impose the necessary boundary conditions (e.g. periodic or open boundary conditions), where particles can move in and out of the system. This is much more difficult in the coordinate representation.

The quantum equation of motion for the density matrix of the system interacting with heat bath is known as the quantum Fokker-Planck equation [1]. We have generalized it to a multi-state system with anharmonic potentials and coordinate-dependent nonadiabatic coupling.

$$\begin{aligned} \frac{\partial}{\partial t} W_{jk}(P, R, t) = & -\frac{P}{M} \frac{\partial}{\partial R} W_{jk}(P, R, t) + \zeta \frac{\partial}{\partial P} \left(P + \frac{M}{\beta} \frac{\partial}{\partial P} \right) W_{jk}(P, R, t) \\ & - \frac{1}{\hbar} \int \frac{dP'}{2\pi\hbar} \sum_m [X_{jm}(P-P', R, t) W_{mk}(P', R, t) \\ & + X_{mk}^*(P-P', R, t) W_{jm}(P', R, t)]. \end{aligned} \quad (9)$$

Here, ζ is the friction constant and

$$X_{jj}(P, R, t) = i \int_{-\infty}^{\infty} dr \exp(iPr/\hbar) U_{jj}(R-r/2, t), \quad (10)$$

$$X_{jj}^*(P, R, t) = -i \int_{-\infty}^{\infty} dr \exp(iPr/\hbar) U_{jj}(R+r/2, t).$$

This equation of motion is valid only when the following high temperature condition applies:

$$\beta \hbar \omega_j \ll 1, \quad (11)$$

where ω_j is a characteristic frequency of the system and $\beta = 1/k_B T$ is the inverse temperature of the environment (bath). This limitation can be relaxed, if we consider a Gaussian-Markovian bath with a finite correlation time [2, 3].

There are several possible strategies for computing the optical signal. The first is based on a perturbative expansion of the density matrix in the entire electromagnetic field $E_p + E_r$. In this procedure the signal is expressed in terms of multitime correlation functions of the dipole operator, which constitute the nonlinear response functions [4]. This procedure is particularly useful for weak fields and it has been applied to a wide range of experiments such as the pump-probe or coherent Raman spectroscopy. The second method involves a direct integration of the equations of motion with all fields present. The third approach is intermediate between the two. We assume weak probe and expand the density matrix to linear order in E_r . We then get

$$P(r, t) = -\frac{i}{\hbar} \int_{-\infty}^t dt' \langle \mu^0(t), \mu^0(\tau) | P_{\text{opt}} > E_r(\mathbf{r}, \tau), \quad (12)$$

where,

$$\mu^0(t) \equiv \exp\left\{ \frac{i}{\hbar} \int_0^t dt' H_A^0(\tau) \right\} \mu(R) \exp\left\{ -\frac{i}{\hbar} \int_0^t dt' H_A^0(\tau) \right\}, \quad (13)$$

and $H_A^0(t)$ is the Hamiltonian without the probe field (Eq.(2) with $E_r(\mathbf{r}, t) = 0$) and P_{opt} is the equilibrium density matrix.

A technical difficulty with this calculation is the necessity to select the polarization with the given wavevector. Formally atoms located in the different positions will see the optical fields with different phases ($\cos(\omega t - \mathbf{k} \cdot \mathbf{r})$). For non-interacting atoms, the integration over \mathbf{r} is equivalent to solving the problem repeatedly for various phases of the fields and then averaging over the phases, thereby selecting the desired wavevector component. This procedure is computationally intensive but in some cases it may be possible to avoid it by a suitable transformation [5].

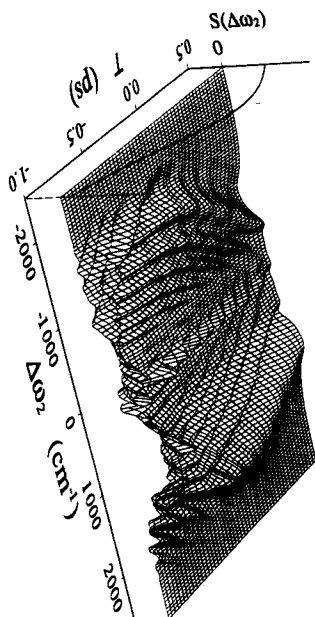


Fig. 1 Pump-probe spectrum of a two-level system subjected to a strong excitation for different pulse delays T [ps] and probe dispersed frequency $\Delta\omega_2$. The nuclear degree of the freedom R is modelled as an underdamped Brownian oscillator with the following parameters: frequency $\omega_0=500[\text{cm}^{-1}]$ and friction $\gamma=50[\text{cm}^{-1}]$. Its equilibrium position is linearly displaced between the two-electronic states with the dimensionless displacement $D=1$, and the temperature $T=200[\text{K}]$. We assumed that both the pump and probe pulses are Gaussian $E_1(t)=E_1\exp[-(t/\tau_1)^2]$ and $E_2(t)=E_2\exp[-(t-T)/\tau_2]^2$ with resonance central frequencies, *i.e.* $\Omega_1=\Omega_2=\omega_{rg}$, where ω_{rg} is the electronic transition frequency of the two-level system. The pulse durations were taken to be $\tau_1=700[\text{fs}]$ and $\tau_2=30[\text{fs}]$ and the time delay was varied between $T=-2[\text{ps}]$ to $T=0.5[\text{ps}]$. The trace above the T axis shows the pump envelope. The dynamical Stark effect shows up when the pump and the probe overlap in time [5].

The support of the National Science Foundation and the Air Force Office of Scientific Research is gratefully acknowledged.

1. A. O. Caldera and A. J. Leggett, *Physica* **121A**, 587 (1983).
2. Y. Tanimura and S. Mukamel, submitted to *J. Chem. Phys.*
3. Y. Tanimura and P. G. Wolynes, *J. Chem. Phys.* **96**, 8485 (1992).
4. Y. J. Yan and S. Mukamel, *Phys. Rev. A* **41**, 6485 (1990).
5. Y. Tanimura and S. Mukamel, *J. Phys. Soc. Jpn.* **63**, 66 (1994).